Millennial-scale surface and subsurface paleothermometry from the northeast Atlantic, 55–8 ka BP

V. L. Peck,[1,2] I. R. Hall,[1] R. Zahn,[3] and H. Elderfield[4]

Received 3 April 2008; revised 16 June 2008; accepted 27 June 2008; published 24 September 2008.

[1] We present high-resolution records of upper ocean temperatures derived from Mg/Ca ratios of surface-dwelling *Globigerina bulloides* and subsurface-dwelling *Neogloboquadrina pachyderma* sinistral and the relative abundance of *N. pachyderma* sinistral for the period 55–8 ka BP from NE Atlantic sediment core MD01-2461. Millennial-scale temporal variability and longer-term trends in these records enable us to develop a detailed picture of past ocean conditions such as a weakening of thermocline intensity from marine isotope stage 3 (MIS 3) to the last glacial maximum (LGM). The correspondence of all temperature proxies and convergence of paired oxygen isotope ($\delta^{18}O$) records from both planktonic species implies a breakdown in the thermocline and year-round mixing of the upper water column through the LGM, perhaps related to decreasing insolation and additional cooling in association with the expansion of the circum–North Atlantic ice sheets. Millennial-scale divergence in surface and subsurface temperatures and $\delta^{18}O$ across the last glacial correspond to meltwater release and the development of a strong halocline associated with both Heinrich (H) events and instabilities of the NW European ice sheet. During such episodes, *G. bulloides* Mg/Ca appears to record ambient, even warming summer sea surface temperatures across H events while the other proxies record maximum cooling.

Citation: Peck, V. L., I. R. Hall, R. Zahn, and H. Elderfield (2008), Millennial-scale surface and subsurface paleothermometry from the northeast Atlantic, 55–8 ka BP, *Paleoceanography*, *23*, PA3221, doi:10.1029/2008PA001631.

1. Introduction

[2] To date, reconstructions of surface-ocean conditions for the glacial North Atlantic are largely based on planktonic foraminiferal census counts, with sea surface temperature (SST) estimated from the transfer function technique (TFT [*Imbrie and Kipp*, 1971]) or the modern analog technique (MAT [*Prell*, 1985]), forming the most comprehensive picture of last glacial maximum (LGM) conditions (*CLIMAP Project Members* [1981] and GLAMAP 2000 [*Pflaumann et al.*, 2003]). With the advent of temperature-sensitive organic biomarkers and trace metal ratios in foraminiferal shells as tools to infer paleo-SST, a reassessment of the CLIMAP reconstruction of LGM conditions using a multiproxy approach is now possible [*Mix et al.*, 2001; *Kucera et al.*, 2005, *de Vernal et al.*, 2006]. SST estimates derived from multiple proxy approaches yield differing results [e.g., *Nürnberg et al.*, 2000; *Bard*, 2001; *Kandiano et al.*, 2004] highlighting the need for a fuller understanding of the parameters and processes that determine the linking of the SST paleoproxy with ambient temperature, e.g., habitat depth, growth season and preferred temperature range of the particular organism that serves as the signal carrier. Paired, multiproxy SST records from the same sediment core in conjunction with paired planktonic $\delta^{18}O$ records have the potential to better characterize surface ocean conditions, for example seasonal variability of temperature and upper water column stratification [*Barker et al.*, 2005] provided the proxy-temperature relationship is well constrained. Finally, numerical climate and inverse proxy modeling relies on accurate paleo-SST reconstructions in order to test and refine the predictive skills of the models [e.g., *Schäfer-Neth and Paul*, 2004].

[3] Here we present high-resolution multispecies planktonic foraminiferal Mg/Ca and $\delta^{18}O$ records as a means of determining absolute surface and subsurface temperatures from the NE Atlantic between 55 and 25 ka BP. These data extend the 25–8 ka BP paleoenvironmental records for site MD01-2461 reported by *Peck et al.* [2006] allowing upper ocean conditions to be assessed over the interval 55–8 ka BP. We compare the Mg/Ca-derived temperature records with the relative abundance of the polar planktonic foraminiferal species *Neogloboquadrina pachyderma* sinistral, a proxy for the relative contribution of polar water masses and a primary driver of TFT and MAT based SST estimates at high latitude [e.g., *Maslin et al.*, 1995; *Madureira et al.*, 1997; *Kandiano and Bauch*, 2003]. Coupled with records of ice sheet instability from the same core, we interpret the environmental conditions that these two proxy approaches recorded during the last glacial.

2. Material and Methods

[4] Sediment core MD01-2461 was recovered from the northwestern flank of the Porcupine Seabight (51°45′N, 12°55′W) in a water depth of 1153 m (Figure 1). Chronology of MD01-2461 is based on 25 ^{14}C AMS dates

[1]School of Earth and Ocean Sciences, Cardiff University, Cardiff, UK.
[2]Now at British Antarctic Survey, Cambridge, UK.
[3]Institució Catalana de Recerca i Estudis Avançats and Institut de Ciència i Tecnologia Ambientals, Departament de Geologia, Universitat Autònoma de Barcelona, Bellaterra, Spain.
[4]Department of Earth Sciences, Cambridge University, Cambridge, UK.

0883-8305/08/2008PA001631

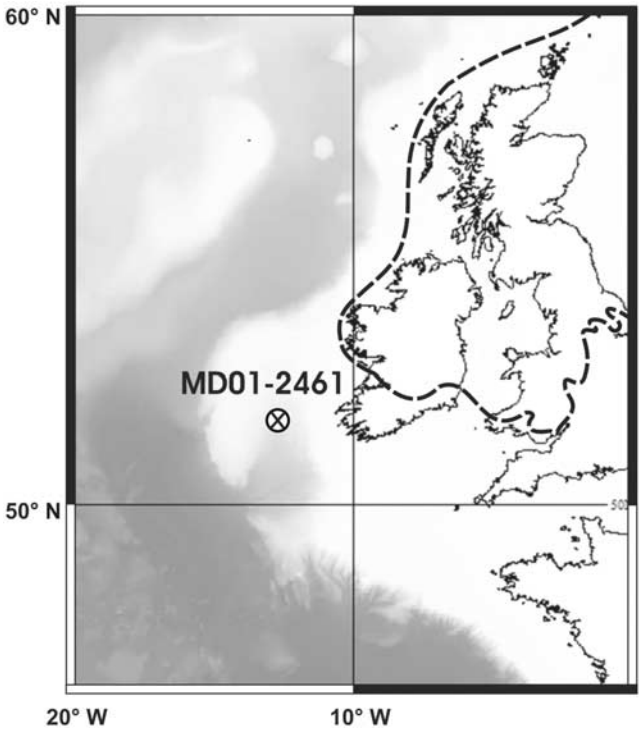

Figure 1. Location of core MD01-2461 in the NE Atlantic. Dashed line indicates limit of the last glacial British ice sheet.

calibrated to calendar years before present (years BP) using CALIB 5.0.1 (with MARINE04) and the subsequent fine tuning of the abundance record of *N. pachyderma* sinistral to the GISP2 $\delta^{18}O_{ice}$ record [*Peck et al.*, 2007] (Figures 2a and 2b). Correlation between the two records is robust over their total length (1.2–9.5 m core depth, 8–55 ka BP) to within r = 0.70, increasing to r = 0.84 between 25 and 8 ka BP as temporal resolution in the marine record increases across the LGM and the last deglacial.

[5] Fine-scale records of ice rafted debris (IRD) provenance and flux (grains > 150 μm cm^{-2} ka^{-1}) from MD01-2462 [*Peck et al.*, 2006, 2007] detail the history of growth and variability of the NW European ice sheets (NWEIS, comprising the British, Icelandic and Fennoscandian ice sheets), and the Heinrich (H) events [*Heinrich*, 1988; *Broecker*, 1994] defined by the catastrophic collapse of the Laurentide ice sheet (LIS).

[6] Upper water column conditions are determined through paired Mg/Ca and $\delta^{18}O$ analysis of surface-dwelling *Globigerina bulloides* and subsurface-dwelling *N. pachyderma* sinsitral.

[7] *G. bulloides* today calcifies in the upper 60 m of the water column [e.g., *Schiebel et al.*, 1997]; within this paper we assume that Mg/Ca and stable isotope values are representative of a mean calcification depth of 30 m [cf. *Barker and Elderfield*, 2002] and a preferred summer growth season centered on July [*Hillaire-Marcel and Bilodeau*, 2000; *Peck et al.*, 2006]. *N. pachyderma* sinistral inhabit a broad range of water depths. Juvenile forms occupy relatively shallow waters (~50 to 80 m) and migrate to 500–600 m depth during ontogeny, spending much of their lives within the pycnocline [*Carstens et al.*, 1997; *Bauch et al.*, 1997; *Hillaire-Marcel and Bilodeau*, 2000]. We assume a mean calcification depth for *N. pachyderma* sinistral of ~150 m, reflecting the depth of peak *N. pachyderma* sinistral concentrations in modern subpolar waters [*Kohfeld et al.*, 1996; *Carstens et al.*, 1997; *Volkmann*, 2000; *Simstich et al.*, 2003]. Below the thermocline there is little seasonal variability of water temperatures, such that oxygen isotope and Mg/Ca values derived from *N. pachyderma* sinistral are likely to reflect mean annual subsurface conditions at ~150 m [cf. *Nürnberg*, 1995].

2.1. Trace Element and Stable Isotope Analysis

[8] For paired stable isotope and Mg/Ca analysis of both planktonic species, 50 specimens were selected wherever possible, with the minimum number of individuals used being 20. *G. bulloides* specimens were selected from the 250–315 μm size fraction and *N. pachyderma* sinistral from the 150–250 μm size fraction. These narrow size fractions minimize variability in stable isotope and Mg/Ca measurements that may arise from varying chamber numbers/test size [*Spero and Lea*, 1996] and restricts the likely habitat depth interval within which the specimens calcified [*Kroon and Darling*, 1995]. Average test weights were monitored using a high-precision top pan balance in order to identify any changes in test wall thickness down core, which may be indicative of carbonate dissolution. Specimens were then crushed between glass slides to break open the chambers to release possible sediment infill, shell fragments were homogenized and aliquots taken for paired Mg/Ca and stable isotope analyses.

[9] For stable isotope analysis, 50% of the sample was immersed in 3% hydrogen peroxide for 30 min and ultra-

Figure 2. Climate, upper ocean temperatures, and ice sheet activity as recorded at MD01-2461. (a) GISPII $\delta^{18}O$ ice core record. High-resolution $\delta^{18}O_{ice}$ record (five-point smoothed) from the Greenland summit GISPII ice core (http://depts.washington.edu/qil/datasets/gisp2_main.html) [*Grootes and Stuiver*, 1997]. (b) *N. pachyderma* sinistral %. (c) $Mg/Ca_{G.\ bulloides}$. The secondary axis indicates SST determined from *Pak et al.* [2004] on the left and *Peck et al.* [2006] on the right in bold. Core top $Mg/Ca_{G.\ bulloides}$ shown by red dashed line. (d) $Mg/Ca_{N.\ pachyderma\ sinistral}$ The secondary axis indicates subsurface water temperature determined from *Nürnberg et al.* [1996] (Norwegian Sea core top calibration) on the left and *Peck et al.* [2006] on the right in bold. (e) Oxygen isotope records of *G. bulloides* (red) and *N. pachyderma* sinistral (blue) (‰ VPDB). (f) Sedimentation rate. (g) Flux of total IRD to the core site. (h) Flux of LIS-sourced dolomitic carbonate to the core site (>150 μm cm^{-2} a^{-1}). Radiocarbon dates indicated by black triangles. Tie points between GISPII $\delta^{18}O$ and MD01-2461 *N. pachyderma* sinistral % fine tune the cores chronology. Orange bands locate H events H1, H2, H4, and H5. Purple bands locate Icelandic debris of H3 and the Younger Dryas. Brown bands locate two episodes of increased BIS debris flux at the LGM.

sonicated in methanol for 15 s before excess liquid and residue was removed and the sample dried at 45°C. All stable isotope analyses were made using a ThermoFinnigan MAT 252 and Kiel II automated carbonate preparation device with an external reproducibility of $\leq$0.08‰ for $\delta^{18}O$. Stable isotope values are reported on the VPDB scale, calibrated through the international NBS 19 carbonate standard.

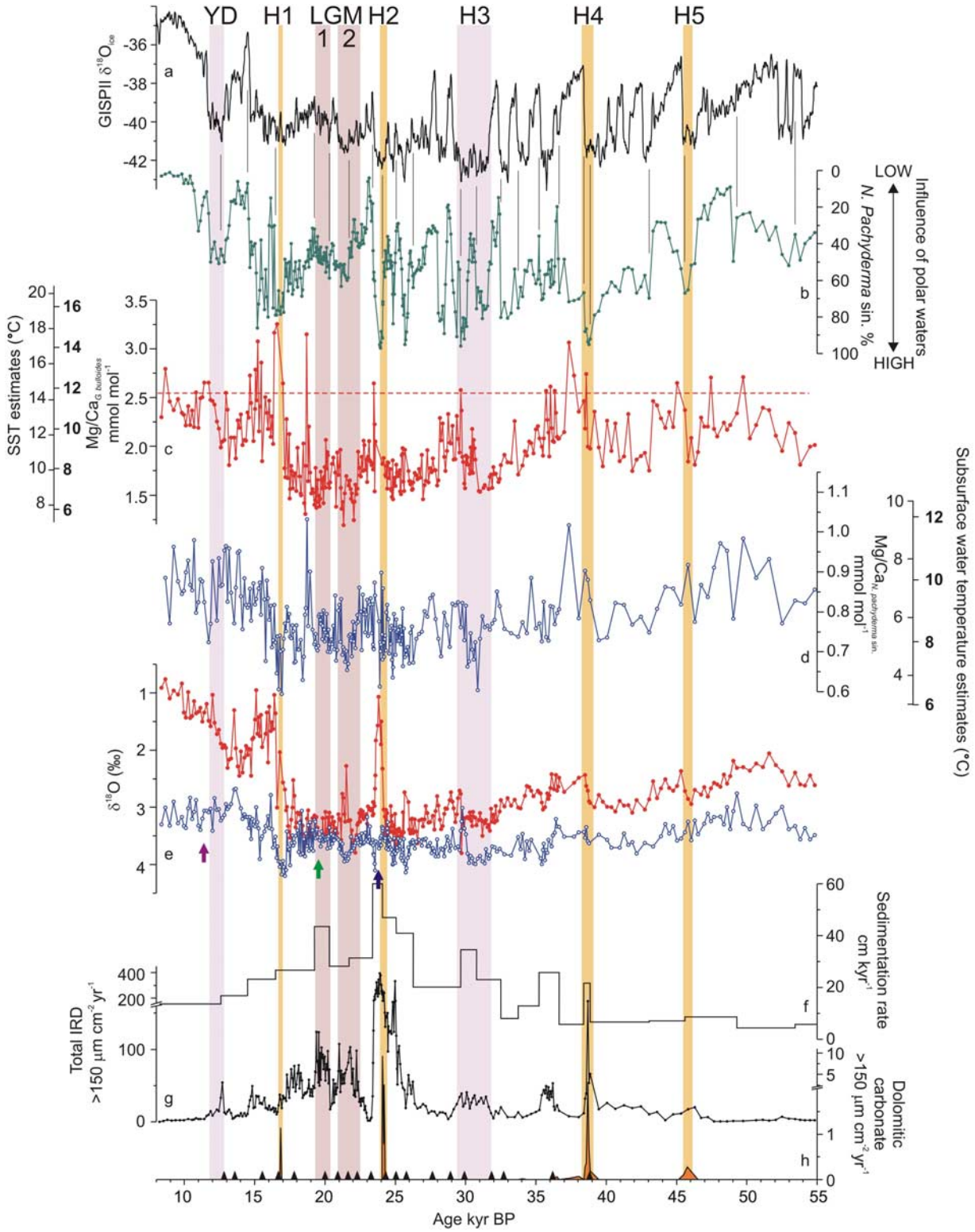

Figure 2

[10] The sample aliquot for Mg/Ca analysis was cleaned following *Barker et al.* [2003]. Samples were diluted in 0.075 mol HNO_3 to a fixed Ca concentration of 100 ppm where possible, with all samples containing >40 ppm. Analyses were carried out on a Varian Vista ICP-AES. Intensity ratios were calibrated against elemental ratios following *de Villiers et al.* [2002] to eliminate Ca matrix effect. Analytical precision determined from replicate runs of a standard solution of Mg/Ca = 5.130 (60 ppm Ca) and Mg/Ca = 1.289 (100 ppm Ca) was $\leq$0.4% (1σ). Sample reproducibility is <4% as determined from duplicated sample runs.

2.2. Mg/Ca Paleothermometery

[11] Foraminiferal Mg/Ca is a viable temperature proxy but there are several potential complications that need to be considered.

2.2.1. Clay Contamination

[12] The possibility of clay contamination elevating the Mg/Ca ratio [*Barker et al.*, 2003] has been eliminated by discarding samples from the record that contain traceable Al concentrations (>5 ppb in samples where Ca is >80 ppm). 39 measurements (26 or 7% of *G. bulloides*, and 13 or 4% of *N. pachyderma* sinistral) yielding Al concentrations above detection level were discarded from a total of 706 measurements.

2.2.2. Contamination From Dolomitic Carbonate and/or Volcanic IRD

[13] Mg contamination from the discrete dolomitic carbonate-rich horizons deposited during H events (or volcanic debris in the case of H3) would presumably affect the Mg/Ca both species similarly such that simultaneous increases in Mg/Ca of both *G. bulloides* and *N. pachyderma* sinistral associated with these events would be diagnostic of this contamination. However, dissimilar, even anti-phased, trends in Mg/Ca records of the two species are observed across each event discrediting IRD as a source of Mg contamination.

2.2.3. Salinity Changes

[14] Laboratory cultures suggest that salinity changes in ambient seawater influences foraminiferal Mg uptake, Mg/Ca of foraminiferal calcite decreasing with reducing salinity [*Nürnberg et al.*, 1996; *Lea et al.*, 1999]. Assuming a stable depth habitat, reduced salinity in the course of the H event meltwater surges would therefore cause an underestimation of temperatures derived from *G. bulloides* living with the halocline. $Mg/Ca_{G.\ bulloides}$ maintains ambient to elevated Mg/Ca ratios across H meltwater events suggesting that temperature, not salinity, is the dominant control on Mg/Ca in these circumstances.

2.2.4. Dissolution

[15] Dissolution of foraminiferal calcite reduces Mg/Ca, leading to an underestimation of calcification temperature [*Rosenthal et al.*, 2000]. The site of MD01-2461 at 1153 m water depth was well above the lysocline throughout the last glacial cycle. All tests used for analysis were well preserved. The average test weights were *G. bulloides* and *N. pachyerma* sinistral were 15.0 ± 1.7 (n = 46) and 9.8 ± 1.2 (n = 45) μg respectively. The limited range of variability ($\sim$12%) supports good preservation [*Barker and Elderfield*, 2002].

[16] Taking these considerations into account we feel it unlikely that secondary effects exerted measurable control on the Mg/Ca records and hence are convinced the records provide reliable indications of SST variability.

2.3. Mg/Ca Temperature Calibrations

[17] To date, the few Mg/Ca T calibrations that have been established for SST < 10°C [*Barker and Elderfield*, 2002] are restricted to the region within which the calibration was determined, producing unfeasible temperature estimates outside the calibration area [e.g., *Kandiano et al.*, 2004]. The calibrations used in this study [*Peck et al.*, 2006] fall at the cooler and warmer extremes of the calibration spectra for *G. bulloides* and *N. pachyderma* sinistral respectively (Figure 2). They were determined via core top calibration of *G. bulloides* assuming Mg/Ca temperature sensitivity of 10% $°C^{-1}$ [*Peck et al.*, 2006] and for *N. pachyderma* sinistral using the assumption that similar calcification temperatures are recorded by both species at the LGM (20–19 ka BP; Figure 2), when both species display virtually identical $\delta^{18}O$ values, and the same Mg/Ca temperature sensitivity of 10% $°C^{-1}$. Applying the Southern temperature calibration of *Mashiotta et al.* [1999] to our Mg/Ca record of *G. bulloides* yields glacial SST estimates that are up to 13°C higher than faunal based SST estimates, consistent with similar observations of *Kandiano et al.* [2004]. Cooler temperatures derived from our calibration likely reflect the fact that in this study core top samples are calibrated to temperatures at 30 m water depth, the mean calcification depth of *G. bulloides*. Support for the *G. bulloides* Mg/Ca temperature calibration presented by *Peck et al.* [2006] is the marginally cooler calibration ($\sim$0.57°C offset) of *Barker and Elderfield* [2002] derived from a North Atlantic core top at $\sim$60°N, reinforcing the suggestion that significantly different Mg/Ca temperature relationships exist between North and South Atlantic for *G. bulloides* (although a Mg/Ca temperature sensitivity of 10% $°C^{-1}$ is persistent).

[18] At present, *N. pachyderma* sinistral is restricted in the North Atlantic to latitudes north of $\sim$60° N [*Pflaumann et al.*, 1996], preventing core top validation of the Mg/Ca temperature relation of this species at site MD01-2461. The relatively warm glacial temperatures predicted from the *Peck et al.* [2006] calibration for *N. pachyderma* sinistral exhibiting +2.9°C and +0.8°C average offset compared to Norwegian Sea and Southern Ocean core top-derived calibrations respectively [*Nürnberg et al.*, 1996], may also reflect regional/latitudinal variability in calibrations, perhaps relating to genotype variability [*Darling et al.*, 2000; *Kucera and Darling*, 2002]. Using the previously published Mg/Ca temperature calibrations and combining them with paired foraminiferal $\delta^{18}O$ at MD01-2461 results in temperature and salinity that do not fulfill the requirement of neutral or stable upper ocean stratification [*Peck et al.*, 2006]. Such considerations further highlight the necessity of species and region specific calibration.

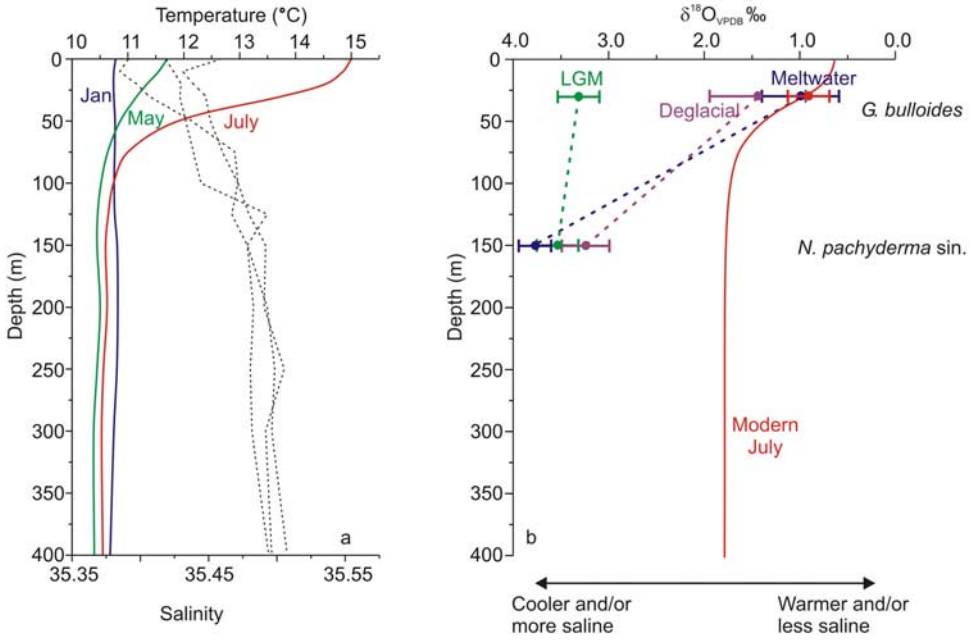

Figure 3. Upper water column temperature, salinity, and $\delta^{18}O$ of equilibrium calcite at the site of MD01-2461. (a) Modern temperature and salinity for January, May, and July and (b) equilibrium calcite for modern July conditions (red), calculated using the paleotemperature equation of *Shackleton* [1974] and the modern North Atlantic δ_w-salinity relationship, $\delta_w = S \times 0.61 - 21.3$ [*United Nations Educational, Scientific and Cultural Organization*, 1980]. Red data point with error bar shows core top $\delta^{18}O_{G.\ bulloides}$ at the average depth habitat of *G. bulloides* (30 m). Deglacial conditions (purple) use average $\delta^{18}O$ of both *G. bulloides* and *N. pachyderma* sinistral across the interval 13–10 ka BP, LGM conditions (green) from 20 to 19 ka BP, and meltwater event example from H2 (blue), 24 ka BP. *N. pachyderma* sinistral data plotted at average depth habitat of 150 m. Selected time intervals are indicated on Figure 2e.

2.4. Faunal Counts

[19] The relative abundance of the polar species *N. pachyderma* sinistral is a paleoindicator of polar waters [*Bé*, 1977; *Reynolds and Thunell*, 1985; *Johannessen et al.*, 1994; *Pflaumann et al.*, 1996, 2003]. In waters of summer SST < 8°C, this species dominates the planktonic foraminiferal assemblage [*Pflaumann et al.*, 1996] such that TFT SST estimates are significantly determined by the relative abundance of *N. pachyderma* sinistral within this region [*Kandiano and Bauch*, 2003].

[20] A minimum of 300 planktonic foraminiferal shells were counted from sample splits >150 μm [*CLIMAP Project Members*, 1976, 1984] (standard size fraction) to determine *N. pachyderma* sinistral %. Reproducibility is ±5% of absolute values.

3. Results and Discussion

3.1. Coupled Surface and Subsurface Mg/Ca and Oxygen Isotope Records

[21] Comparison of the $\delta^{18}O$ of surface- and subsurface-dwelling foraminifera serves as an indication of upper water column stratification [*Hillaire-Marcel and Bilodeau*, 2000; *Simstich et al.*, 2003]. Today, at the location of MD01-2461, summer temperatures within the depth habitat range of *G. bulloides* are ~3°C warmer than in the depth range of *N. pachyderma* sinistral [*Levitus*, 1998]. Comparison of calculated $\delta^{18}O$ of equilibrium calcite (Figure 3; calculated using the paleotemperature equation of *Shackleton* [1974] and the modern North Atlantic δ_w-salinity relationship, $\delta_w = S \times 0.61 - 21.3$ [*Craig and Gordon*, 1965]) with core top $\delta^{18}O_{G.\ bulloides}$ from MD01-2461 suggests a summer bloom season (~July). This timing assumes no vital effects on *G. bulloides* $\delta^{18}O$ [*Peck et al.*, 2006], however, previous North Atlantic core top studies have identified a 1°C offset between modern summer SST and isotopic temperatures derived from *G. bulloides* [*Duplessy et al.*, 1991]. Correcting for such a vital effect in our record would increase inferred summer SST, perhaps indicating a later bloom period (e.g., August). The absence of *N. pachyderma* sinistral within the MD01-2461 core top precludes similar assessment of growth season and/or vital effect offset from equilibrium calcite. Deglacial records (~11 ka BP) allow the most recent direct comparison between the two species. The $\delta^{18}O$ offset between the two species at this time suggests a higher gradient between the two habitat depths compared to today, which was overall cooler (by ~1°C as suggested by $Mg/Ca_{G.\ bulloides}$) and more saline. At the LGM (19–20 ka BP), the $\delta^{18}O$ records of the two species converge suggesting an absence of a well-developed seasonal thermocline and enhanced vertical mixing of the upper water column throughout the year. Millennial-scale events are also clearly identified within the $\delta^{18}O$ records, with amplitudes of

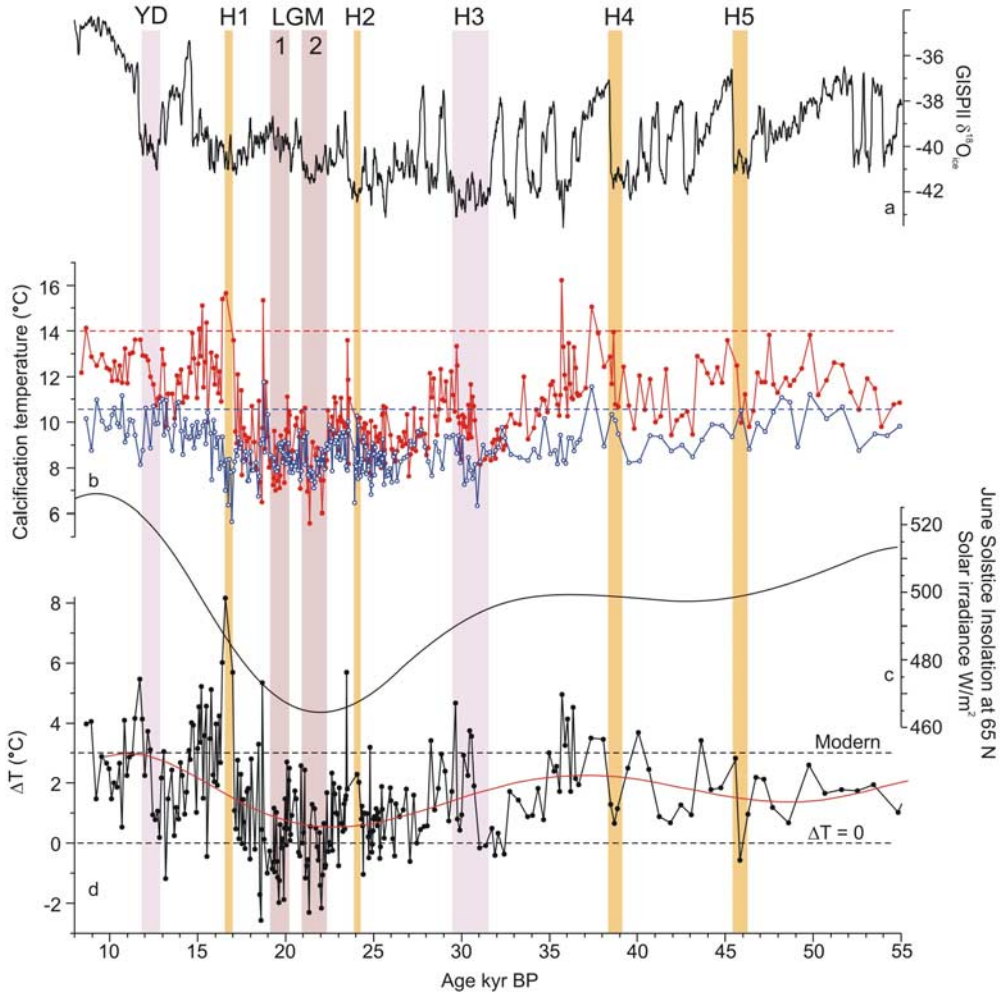

Figure 4. Temperature estimates and seasonality of the upper water column at MD01-2461 over the last 55 ka. (a) GISPII δ^{18}O ice core record. (b) Summer SST inferred from Mg/Ca$_{G.\ bulloides}$ (red solid circles) following *Peck et al.* [2006]. Modern summer SST shown by red dashed line. Mean annual subsurface temperature inferred from Mg/Ca$_{N.\ pachyderma\ sinistral}$ (blue open circles) following *Peck et al.* [2006]. Modern mean annual water temperature at 150 m shown by blue dashed line. (c) June solstice solar insolation at 65°N (La90) [*Laskar*, 1990]. (d) ΔT (summer subsurface temperature (SST), °C). A 6th-order polynomial fit is shown in red. Modern ΔT and ΔT = 0 shown with dashed lines.

divergence between the paired δ^{18}O profiles exceeding 3 ‰ at H2 (Figure 2e), suggesting significant freshening and/or warming of the surface layer while subsurface waters became cooler and/or more saline.

[22] Some millennial-scale anomalies are not recorded in parallel in the δ^{18}O or Mg/Ca proxy records from the same species (e.g., Figure 2, at 22–21 ka BP, *G. bulloides* and at 18.8 ka BP, both species), reflecting the salinity component of the δ^{18}O record.

[23] Temperatures derived from Mg/Ca$_{G.\ bulloides}$ suggest variation of summer SST (at 30 m water depth) within the range between 7 and 14°C, with occasional brief excursions beyond these limits, compared with modern summer SST (at 30 m) of 14°C [*Levitus*, 1998] (Figure 4b). Broad summer SST trends derived from *G. bulloides* are largely reproduced in mean annual subsurface temperatures (~150 m water depth), as determined from Mg/Ca$_{N.\ pachyderma}$ sinistral, within the range 7–11°C, again with occasional brief excursions beyond these limits (Figure 4b). Additionally, down core offsets in the summer SST and mean annual subsurface records of *G. bulloides* and *N. pachyderma* sinistral respectively (ΔT; Figure 4e) plausibly indicate variation in the seasonal thermocline intensity in conjunction with orbitally paced changes in insolation, as is suggested by the visual correlation between ΔT and 21 June insolation at 65°N lagged by 2 ka (Figure 4d).

3.2. Mg/Ca and Faunal Indicator Records

[24] Using the *N. pachyderma* sinistral % summer SST calibration of *Pflaumann et al.* [1996], absolute values of last glacial to deglacial summer SSTs are derived from the *N. pachyderma* sinistral % record. Comparison with the summer SST record derived from Mg/Ca$_{G.\ bulloides}$ (Figure 5a) reveals temporal inconsistencies in temperature trends

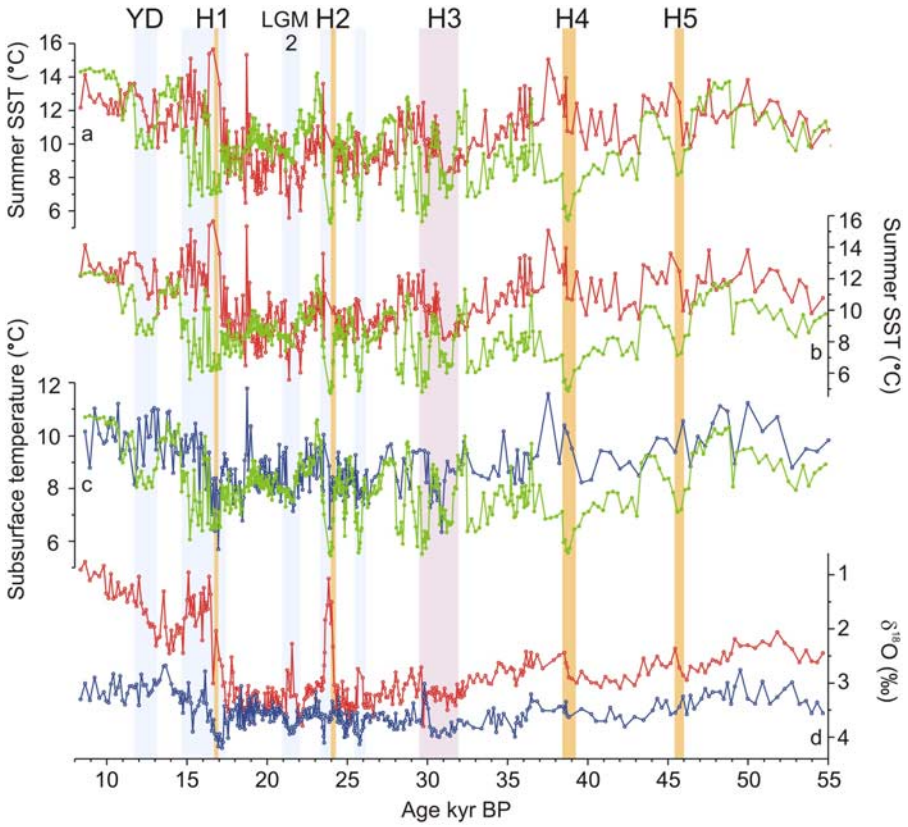

Figure 5. Comparison of surface and subsurface Mg/Ca temperature records with *N. pachyderma* sinistral %-derived temperatures. (a) *N. pachyderma* sinistral % summer SST (calibrated following *Pflaumann et al.* [1996], green) and $Mg/Ca_{G.\ bulloides}$-derived summer SST (red). (b) *N. pachyderma* sinistral % temperature record rescaled to water temperatures at ~30 m water depth through linear interpolation of earliest Holocene and LGM (22–21 ka BP); summer SST = 12.5 − 0.08 × *N. pachyderma* sinistral % with $Mg/Ca_{G.\ bulloides}$-derived summer SST (red). (c) Rescaling of the *N. pachyderma* sinistral % temperature calibration (subsurface temperature = 11 − 0.048 × *N. pachyderma* sinistral %) with $Mg/Ca_{N.\ pachyderma\ sinistral}$-derived subsurface temperature (blue). (d) $\delta^{18}O$ records of *G. bulloides* (red) and *N. pachyderma* sinistral (blue) (‰ VPDB). Orange bands locate H events H1, H2, H4, and H5. H3 indicated by purple band. Meltwater stratification events highlighted by blue bands.

between these two approaches while the absolute temperature range predicted by each proxy is similar. Consistent with the structure of the *N. pachyderma* sinistral % record the derived SST profile displays high-frequency variability at higher amplitudes than is seen in the $Mg/Ca_{G.\ bulloides}$ derived SST profile (Figures 5a and 5b). The correlation coefficient (r) between *N. pachyderma* sinistral % and $Mg/Ca_{G.\ bulloides}$ temperatures is 0.12, although it should be noted that r = 0.37 in the period 28–8 ka BP. Perhaps unsurprisingly, a closer correlation is observed between the *N. pachyderma* sinistral %-derived temperatures and $Mg/Ca_{N.\ pachyderma\ sinistral}$ records with a correlation coefficient of 0.35. Rescaling of the *N. pachyderma* sinistral % temperature calibration to the $Mg/Ca_{N.\ pachyderma\ sinistral}$-derived subsurface temperatures (subsurface temperature = 11–0.048 × *N. pachyderma* sinistral %) illustrates the correlation of the two profiles particularly well especially during the period 28–8 ka BP when r = 0.45 (Figure 5c).

3.3. Upper Ocean Conditions 55–26.5 ka BP

[25] Prior to ~35 ka BP, summer SST inferred from the $Mg/Ca_{G.\ bulloides}$ record, average 11.7 ± 1.2°C with several intervals approaching or exceeding modern summer SST (~14°C [*Levitus*, 1998]) (Figure 4b). Within this period, $Mg/Ca_{G.\ bulloides}$-derived temperatures are on average 1.7°C warmer than $Mg/Ca_{N.\ pachyderma\ sinistral}$ temperatures, concurrent with an average interspecies $\delta^{18}O$ offset of 0.7 ‰ (Figure 2e). These data suggest the development of a seasonal thermocline at this site weaker than that which develops today, perhaps reflecting reduced solar insolation at this time (Figure 4d). Prominent % *N. pachyderma* sinistral maxima during H5 and H4 signify maximum cooling that is not replicated in the Mg/Ca records.

[26] Approaching H3, ~31.5 ka BP, surface ocean conditions deteriorate with $Mg/Ca_{G.\ bulloides}$ summer SST decreasing to LGM values, ~8.6°C, associated with the apparent breakdown of the seasonal thermocline suggested by ΔT falling to 0°C (Figure 4d).

3.4. LGM to Deglacial Conditions and the British Ice Sheet

[27] Expansion of the proximal British Ice Sheet (BIS) and establishment of extensive marine ice margins is likely to account for a stepped increase in IRD flux to the core site at 26.5 ka BP (Figure 2h) [*Peck et al.*, 2006] concurrent with widespread Northern Hemisphere glacial advance [*Hemming and Hajdas*, 2003]. These enhanced glacial conditions are associated with converging upper ocean temperature estimates and $\delta^{18}O$ from *G. bulloides* and *N. pachyderma* sinistral suggesting a year-round, well-mixed upper water column throughout much of the LGM. This apparent lack of seasonality may reflect minimal insolation at this time. Surface and subsurface temperatures fluctuate within the range 6–10°C during this period, up until ~17.5 ka BP when IRD deposition decreases. The upper ocean temperature estimates predicted by all three proxies appear surprisingly high considering the proximity of our core site to the BIS that reached its maximum extent at ~22 ka BP [*Bowen et al.*, 2002]. Mean annual atmospheric temperatures of ~5°C today define the climatic limit of ice sheet existence [*Vaughan and Doake*, 1996]. $Mg/Ca_{G.\ bulloides}$-derived SST at MD01-2461 of 6–10°C exceed this threshold temperature significantly suggesting LGM climatic conditions were not conducive to BIS stability. This is supported by the elevated IRD flux to the core site during the LGM (Figure 2g) and may indeed reflect a metastable character of the BIS at this time, in which warm surface waters ensured a constant moisture source and surface ice accumulation and caused ablation of the marine ice margin.

[28] Following H1, Mg/Ca-derived temperatures increase and $\delta^{18}O$ values decrease while *N. pachyderma* sinistral % suggests LGM temperatures for a further ~2 ka before warming and converging with the geochemical proxies over the interval 13–14.5 ka BP, the Bölling-Allerød. The Younger Dryas (~12 ka BP) is clearly recorded by elevated *N. pachyderma* sinistral % over a ~1 ka interval, yet no significant cooling signal is apparent in either the Mg/Ca or $\delta^{18}O$ records (Figure 2). This divergence of proxies corresponds to a period of increasing insolation and the rapid development of a seasonal thermocline, ΔT increases from <1°C to >3°C across the Younger Dryas. Following the Younger Dryas, summer SST ($Mg/Ca_{G.\ bulloides}$) approaches modern (core top) values and *N. pachyderma* sinistral % tends to zero as temperatures exceed the optimal temperature range of this species [*Duplessy et al.*, 1991]. The youngest Mg/Ca values, ~8 ka BP, are indicative of a seasonal stratification comparable to today with ΔT approaching modern values (3°C).

3.5. Millennial-Scale Events

[29] Increased IRD flux and *N. pachyderma* sinistral dominance (>75%) of the planktonic assemblage document typical Heinrich conditions, i.e., enhanced iceberg melting and maximum sea surface cooling at MD01-2461 (Figures 2a, 2g, and 2h). Discrete minima in $Mg/Ca_{N.\ pachyderma\ sinistral}$ are associated with H 3, 2 and 1 and are consistent with *N. pachyderma* sinistral % maxima during these events. However, H events do not stand out as prominent cooling events within the $Mg/Ca_{G.\ bulloides}$ summer SST record. With the exception of H5, ambient or even elevated $Mg/Ca_{G.\ bulloides}$ values are observed across each H event, the latter particularly well developed at H1. Divergence of the $Mg/Ca_{G.\ bulloides}$ from both *N. pachyderma* sinistral % and $Mg/Ca_{N.\ pachyderma\ sinistral}$ at H1 and H3 is unexpected, the latter proxies suggesting reduced mean annual temperatures while $Mg/Ca_{G.\ bulloides}$ suggests ambient and even warmer summer SST. Given that the apparent calcification temperature of *G. bulloides* is well within the optimal temperature range of this species during H1, the low abundance of *G. bulloides* coincident with the exceptionally warm summer SST derived from $Mg/Ca_{G.\ bulloides}$ is a paradox. If the longer-term divergence of the paired proxy records prior to H3 indicates enhanced seasonality, could a similar scenario apply to the H1 meltwater surges? Summer SST < 8°C that is implied by a *N. pachyderma* sinistral abundance of >75% in the planktonic foraminifera assemblage suggests conditions outside the optimum environment for *G. bulloides* during the H events. While these surface ocean conditions were likely representative of the majority of years within a given sample interval, accounting for the dominance of polar species *N. pachyderma* sinistral within the planktonic assemblage, summer SST > 10°C recorded in $Mg/Ca_{G.\ bulloides}$ is robust and cannot be ignored. These elevated summer SST may represent a small percentage of mild summers, perhaps even exceptionally warm in the case of H1. Additionally, meltwater events have the potential to enhance seasonality of the upper water column by virtue of a strong, shallow halocline that suppresses vertical exchange with cold subsurface waters and enhances the residence time of surface waters with in the sunlit zone. Upper ocean stratification at MD01-2461 during H1 and H2 contrasts with concurrent intensification of vertical mixing documented in the open North Atlantic on the margins of the IRD belt reflecting stormier conditions in the North Atlantic region during H events [*Rashid and Boyle*, 2007].

[30] Meltwater stratification of the upper water column at MD01-2461 is again evident between 21.6 and 21.0 ka BP where paired $\delta^{18}O$ diverge by >1.5 ‰, coincident with IRD event LGM2 (Figure 2e). Unlike stratification at H1 however, $Mg/Ca_{G.\ bulloides}$ records some of the coldest summer SSTs of the entire record. *N. pachyderma* sinistral % (<60%) suggest ambient glacial SSTs. Occasional negative ΔT values, of up to −2°C (Figure 4d), suggest inversion of the thermocline coincident with enhanced IRD flux and insolation minima, perhaps similar to the cold halocline layer of the Arctic Ocean [*Björk et al.*, 2002]. The relatively cold SSTs associated with BIS ice calving at this time are consistent with glacier advance during LGM cooling [*Bowen et al.*, 2002]. Comparison of $Mg/Ca_{G.\ bulloides}$ records during this BIS ice-rafting event with records spanning meltwater events associated with H events 1 and 2 suggests that ocean-climate conditions connected with collapse of the LIS were different, apparently milder, if not warm, during the summer months.

[31] Very few glacial Mg/Ca SST records have yet been produced in the temperate North Atlantic, most paleo-SST records in the region are derived from faunal census counts. Warm summer SSTs during some H events have not been

recorded in the *N. pachyderma* sinistral record presented here, presumably because faunal census records do not capture this warming but rather display peak maxima of cold faunal components such as *N. pachyderma* sinistral The warming recorded, including exceptionally warm SSTs at H1, may represent just a small percentage of years within a given time interval, the resolution provided by faunal diversity reconstructions prohibiting identification of such anomalous years. If confirmed, mild summer SST, perhaps even at increased levels as suggested from $Mg/Ca_{G.\ bulloides}$ SST records of MD01-2461, may provide support for climatically forced catastrophic disintegration of ice shelves fringing the LIS, and other circum–North Atlantic ice sheets, initiating H events [*Hulbe et al.*, 2004].

[32] Alternatively, transient advections of subtropical surface waters coincident with H events, perhaps driven by the variable strength of a poleward flowing shelf edge current along the European margin [*Kenyon*, 1987] or zonality of low-latitude forcing winds [*McIntyre and Molfino*, 1996], may have carried warm surface waters to the site of MD01-2461, depositing *G. bulloides* carrying anomalously warm Mg/Ca signatures, yet not enough specimens to have influenced the planktonic assemblage record.

4. Summary and Conclusions

[33] In this study, we suggest that $Mg/Ca_{N.\ pachyderma\ sinistral}$ and *N. pachyderma* sinistral % are reliable recorders of mean annual conditions. $Mg/Ca_{N.\ pachyderma\ sinistral}$ recording mean annual temperatures at ~150 m water depth, while *N. pachyderma* sinistral % appears to record mean annual upper ocean temperatures [cf. *Morey et al.*, 2005], rather than summer SST [*Pflaumann et al.*, 1996]. $Mg/Ca_{G.\ bulloides}$ records summer SST.

[34] LGM upper ocean temperatures at MD01-2461 are determined to have been in the range 6–10°C. The proximity of the site to the BIS leads us to propose a metastable character of the BIS at this time, in which warm surface waters ensured a constant moisture source and surface ice accumulation while simultaneously ablating the marine ice margin.

[35] During the last glacial the strength of the seasonal thermocline, determined by ΔT of surface and subsurface waters, is shown to have lagged solar insolation by ~2 ka. The seasonal thermocline began to weaken as insolation decreased from ~35 ka BP, and failed to develop with the expansion of the BIS at ~26.5 ka BP and throughout much of the LGM, until H1 when insolation increased again. All three temperature proxies predict similar paleotemperatures during episodes of year-round mixing of the upper water column, yet quite different conditions when orbital parameters (prior to H3 and the deglacial) or meltwater stratification promote seasonal variability. High-resolution $Mg/Ca_{G.\ bulloides}$ SST records appear to have captured evidence for mild summers, even warming, concurrent with H events, heavily documented in faunal assemblage SST records as representing the coldest intervals of the last glacial. Meltwater stratification and thermal isolation of the surface layer may have accommodated warming of surface waters during a few anomalously warm summers. During the majority of years, however, cool conditions prevailed as recorded in faunal diversity and subsurface temperatures records provided by $Mg/Ca_{N.\ pachyderma\ sinistral}$.

[36] **Acknowledgments.** We thank IPEV and the crew of the R/V *Marion Dufresne* for facilitating the recovery of MD01-2461. We thank R. Chaudri, B. T. Long, and H. J. Medley for assistance with sample preparation; M. Greaves for sharing his expertise in Mg/Ca analysis; and G. G. Bianchi for stable isotope analysis. We are grateful to Laurent Labeyrie and an anonymous reviewer whose comments have greatly improved this manuscript. This work was supported by the Natural Environment Research Council (NERC) and NERC Radiocarbon Laboratory.

References

Bard, E. (2001), Comparison of alkenone estimates with other paleotemperature proxies, *Geochem. Geophys. Geosyst.*, *2*(1), 1002, doi:10.1029/2000GC000050.

Barker, S., and H. Elderfield (2002), Foraminiferal calcification response to glacial-interglacial changes in atmospheric CO_2, *Science*, *297*, 833–836, doi:10.1126/science.1072815.

Barker, S., et al. (2003), A study of cleaning procedures used for foraminiferal Mg/Ca paleothermometry, *Geochem. Geophys. Geosyst.*, *4*(9), 8407, doi:10.1029/2003GC000559.

Barker, S., et al. (2005), Planktonic foraminiferal Mg/Ca as a proxy for past oceanic temperatures: A methodological overview and data compilation for the Last Glacial Maximum, *Quat. Sci. Rev.*, *24*, 821–834, doi:10.1016/j.quascirev.2004.07.016.

Bauch, D., et al. (1997), Oxygen isotope composition of living Neogloboquadrina pachyderma (sin) in the Arctic Ocean, *Earth Planet. Sci. Lett.*, *146*, 47–58, doi:10.1016/S0012-821X(96)00211-7.

Bé, A. W. H. (1977), An ecological, zoogeographic and taxonomic review of recent planktonic foraminifera, in *Oceanic Micropaleontology*, pp. 1–100, Academic, San Diego, Calif.

Björk, G., et al. (2002), Return of the cold halocline layer to the Amundsen Basin of the Arctic Ocean: Implications for the sea ice mass balance, *Geophys. Res. Lett.*, *29*(11), 1513, doi:10.1029/2001GL014157.

Bowen, D. Q., et al. (2002), New data for the Last Glacial Maximum in Great Britain and Ireland, *Quat. Sci. Rev.*, *21*, 89–101, doi:10.1016/S0277-3791(01)00102-0.

Broecker, W. S. (1994), Massive iceberg discharges as triggers for global climate change, *Nature*, *372*, 421–424, doi:10.1038/372421a0.

Carstens, J., et al. (1997), Distribution of planktic foraminifera at the ice margin in the Arctic (Fram Strait), *Mar. Micropaleontol.*, *29*, 257–269, doi:10.1016/S0377-8398(96)00014-X.

CLIMAP Project Members (1976), The surface of the ice-age Earth, *Science*, *191*, 1131–1137, doi:10.1126/science.191.4232.1131.

CLIMAP Project Members (1981), Seasonal reconstructions of the of the earth's surface at the Last Glacial Maximum, *Map Chart Ser.*, *MC-36*, 18 pp., Geol. Soc. of Am., Boulder, Colo.

CLIMAP Project Members (1984), The last interglacial ocean, *Quat. Res.*, *21*, 123–224, doi:10.1016/0033-5894(84)90098-X.

Craig, H., and L. I. Gordon (1965), Deuterium and oxygen 18 variations in the ocean and the marine atmosphere, in *Stable Isotopes in Oceanographic Studies and Paleotemperatures*, edited by E. Tongiorgi, pp. 9–130, Lab. di Geol. Nucl., Cons. Naz. delle Ric., Pisa, Italy.

Darling, K. F., et al. (2000), Molecular evidence for genetic mixing of Arctic and Antarctic subpolar populations of planktonic foraminifers, *Nature*, *405*, 43–47, doi:10.1038/35011002.

de Vernal, A., et al. (2006), Comparing proxies for the reconstruction of LGM sea-surface conditions in the northern North Atlantic, *Quat. Sci. Rev.*, *25*, 2820–2834, doi:10.1016/j.quascirev.2006.06.006.

de Villiers, S., et al. (2002), An intensity ratio calibration method for the accurate determination of Mg/Ca and Sr/Ca of marine carbonates

by ICP-AES, *Geochem. Geophys. Geosyst.*, *3*(1), 1001, doi:10.1029/2001GC000169.

Duplessy, J. C., et al. (1991), Surface salinity reconstruction of the North Atlantic during the Last Glacial Maximum, *Oceanol. Acta*, *4*, 311–324.

Grootes, P. M., and M. Stuiver (1997), Oxygen 18/16 variability in Greenland snow and ice with 10 (−3) to 10 (5)-year time resolution, *J. Geophys. Res.*, *102*, 26,455–26,470, doi:10.1029/97JC00880.

Heinrich, H. (1988), Origin and consequences of cyclic ice-rafting in the Northeast Atlantic ocean during the past 130 000 years, *Quat. Res.*, *29*, 142–152, doi:10.1016/0033-5894(88)90057-97.

Hemming, S. R., and I. Hajdas (2003), Ice-rafted detritus evidence from $^{40}Ar/^{39}Ar$ ages of individual hornblende grains for evolution of the eastern margin of the Laurentide ice sheet since 43 ^{14}C ky, *Quat. Int.*, *99–100*, 29–43, doi:10.1016/S1040-6182(02)00110-6.

Hillaire-Marcel, C., and G. Bilodeau (2000), Instabilities in the Labrador Sea water mass structure during the last climatic cycle, *Can. J. Earth Sci.*, *37*, 795–809.

Hulbe, C. L., et al. (2004), Catastrophic ice shelf breakup as the source of Heinrich event icebergs, *Paleoceanography*, *19*, PA1004, doi:10.1029/2003PA000890.

Imbrie, J., and N. G. Kipp (1971), A new micropaleontological method for quantitative paleoclimatology: Application to a late Pleistocene Caribbean core, in *The Late Cenozoic Glacial Ages*, edited by K. K. Turekian, pp. 71–179, Yale Univ. Press, New Haven, Conn.

Johannessen, T., et al. (1994), The relationship between surface water masses, oceanographic fronts and paleoclimatic proxies in surface sediments of Greenland, Iceland, Norwegian Seas, *NATO ASI Ser.*, *1*(17), 61–85.

Kandiano, E. S., and H. A. Bauch (2003), Surface ocean temperatures in the north-east Atlantic during the last 500 000 years: Evidence from foraminiferal census data, *Terra Nova*, *15*(4), 265–271, doi:10.1046/j.1365-3121.2003.00488.x.

Kandiano, E. S., et al. (2004), Sea surface temperature variability in the North Atlantic during the last two glacial-interglacial cycles: Comparison of faunal, oxygen isotopic, and Mg/Ca-derived records, *Paleogeogr. Paleoclimatol. Paleoecol.*, *204*, 145–164, doi:10.1016/S0031-0182(03)00728-4.

Kenyon, N. H. (1987), Mass-wasting features on the continental-slope of northwest Europe, *Mar. Geol.*, *74*(1–2), 57–77, doi:10.1016/0025-3227(87)90005-3.

Kohfeld, K. E., et al. (1996), Neogloboquadrina pachyderma (sinistral coiling) as paleoceanographic tracers in polar waters: Evidence from Northeast Water Polyna plankton tows, sediment traps, and surface sediments, *Paleoceanography*, *11*, 679–699, doi:10.1029/96PA02617.

Kroon, D., and K. Darling (1995), Size and upwelling control of the stable isotope composition Neogloboquadrina dutertrei (d'Orbigny), Globigerinoides ruber (d'Orbigny), Globigerina bulloides d'Orbigny: Examples from the Panama Basin and Arabian Sea, *J. Foraminiferal Res.*, *25*(1), 39–52.

Kucera, M., and K. F. Darling (2002), Cryptic species of planktonic foraminifera: Their effect on paleoceanographic reconstructions, *Philos. Trans. R. Soc. A*, *360*, 695–718, doi:10.1098/rsta.2001.0962.

Kucera, M., et al. (2005), Multiproxy approach for the reconstruction of the glacial ocean surface (MARGO), *Quat. Sci. Rev.*, *24*, 813–819, doi:10.1016/j.quascirev.2004.07.017.

Laskar, J. (1990), The chaotic motion of the solar system: A numerical estimate of the size of the chaotic zones, *Icarus*, *88*, 266–291, doi:10.1016/0019-1035(90)90084-M.

Lea, D. W., et al. (1999), Controls on magnesium and strontium uptake in planktonic foraminifera determined by live culturing, *Geochim. Cosmochim. Acta*, *63*, 2369–2379, doi:10.1016/S0016-7037(99)00197-0.

Levitus, S. (1998), *World Ocean Atlas*, Natl. Oceanogr. Data Cent., Silver Spring, Md. (Available at http://www.cdc.noaa.gov/)

Madureira, L. A. S., et al. (1997), Late Quaternary high-resolution biomarker and other sedimentary climate proxies in a northeast Atlantic core, *Paleoceanography*, *12*, 255–269, doi:10.1029/96PA03120.

Mashiotta, T. A., et al. (1999), Glacial-interglacial changes in Subantarctic sea surface temperature and delta O-18-water using foraminiferal Mg, *Earth Planet. Sci. Lett.*, *170*, 417–432, doi:10.1016/S0012-821X(99)00116-8.

Maslin, M. A., et al. (1995), Surface water temperature, salinity, and density changes in the northeast Atlantic during the last 45000 years: Heinrich events, deep water formation and climatic rebounds, *Paleoceanography*, *10*, 527–544, doi:10.1029/94PA03040.

McIntyre, A., and B. Molfino (1996), Forcing of Atlantic equatorial and subpolar millennial cycles by precession, *Science*, *274*(5294), 1867–1870, doi:10.1126/science.274.5294.1867.

Mix, A. C., et al. (2001), Environmental processes of the ice age: Land, oceans, glaciers (EPILOG), *Quat. Sci. Rev.*, *20*, 627–657, doi:10.1016/S0277-3791(00)00145-1.

Morey, A. E., et al. (2005), Planktonic foraminiferal assemblages preserved in surface sediments correspond to multiple environment variables, *Quat. Sci. Rev.*, *24*, 925–950, doi:10.1016/j.quascirev.2003.09.011.

Nürnberg, D. (1995), Magnesium in tests of Neogloboquadrina pachyderma sinistral from high northern and southern latitudes, *J. Foraminiferal Res.*, *25*, 350–368.

Nürnberg, D., et al. (1996), Assessing the reliability of magnesium in foraminiferal calcite as a proxy for water mass temperatures, *Geochim. Cosmochim. Acta*, *60*, 803–814, doi:10.1016/0016-7037(95)00446-7.

Nürnberg, D., et al. (2000), Paleo-sea surface temperature calculations in the equatorial east Atlantic from Mg/Ca ratios in planktic foraminifera: A comparison to sea surface temperature estimates from U 37 K′, oxygen isotopes, and foraminiferal transfer function, *Paleoceanography*, *15*, 124–134, doi:10.1029/1999PA000370.

Pak, D. K., et al. (2004), Seasonal and interannual variation in Santa Barbara Basin water temperatures observed in sediment trap foraminiferal Mg/Ca, *Geochem. Geophys. Geosyst.*, *5*, Q12008, doi:10.1029/2004GC000760.

Peck, V. L., et al. (2006), High resolution evidence for linkages between European ice sheet instability and Atlantic meridional overturning circulation, *Earth Planet. Sci. Lett.*, *243*(3–4), 476–488, doi:10.1016/j.epsl.2005.12.023.

Peck, V. L., et al. (2007), The relationship of Heinrich events and their European precursors over the past 60 ka BP: A multi-proxy ice-rafted debris provenance study in the north east Atlantic, *Quat. Sci. Rev.*, *26*(7–8), 862–875, doi:10.1016/j.quascirev.2006.12.002.

Pflaumann, U., et al. (1996), SIMMAX: A modern analog technique to deduce Atlantic sea surface temperatures from planktonic foraminifera in deep-sea sediments, *Paleoceanography*, *11*, 15–35, doi:10.1029/95PA01743.

Pflaumann, U., et al. (2003), Glacial North Atlantic: Sea-surface conditions reconstructed by GLAMAP 2000, *Paleoceanography*, *18*(3), 1065, doi:10.1029/2002PA000774.

Prell, W. L. (1985), The stability of low-latitude sea surface temperatures: An evaluation of the CLIMAP reconstruction with emphasis on the positive SST anomalies, *Tech. Rep., TRO25*, Brown Univ., Providence, R. I.

Rashid, H., and E. A. Boyle (2007), Mixed-layer deepening during Heinrich events: A multi-planktonic foraminiferal $\delta^{18}O$ approach, *Science*, *318*, 439–441, doi:10.1126/science.1146138.

Reynolds, L. A., and R. C. Thunell (1985), Seasonal succession of planktonic foraminifera in the subpolar North Pacific, *J. Foraminiferal Res.*, *15*, 282–301.

Rosenthal, Y., et al. (2000), Incorporation and preservation of Mg in Globigerinoides sacculifer: Implications for reconstructing the temperature and $^{18}O/^{16}O$ of seawater, *Paleoceanography*, *15*, 135–145, doi:10.1029/1999PA000415.

Schäfer-Neth, C., and A. Paul (2004), The Atlantic Ocean at the Last Glacial Maximum: 1. Objective mapping of the GLAMAP sea-surface conditions, in *The South Atlantic in the Late Quaternary: Reconstruction of Material Budgets and Current Systems*, edited by G. Wefer, S. Mulitzer, and V. Ratmeyer, pp. 531–548, Springer, Berlin.

Schiebel, R., et al. (1997), Population dynamics of the planktic foraminifer Globigerina bulloides from the eastern North Atlantic, *Deep Sea Res., Part I*, *44*, 1701–1713, doi:10.1016/S0967-0637(97)00036-8.

Shackleton, N. J. (1974), Attainment of isotopic equilibrium between ocean water and the benthonic foraminifer genus Uvigerina: Isotopic changes in the ocean during the last glacial, *Colloq. CNRS Cent. Natl. Rech. Sci. Paris*, *219*, 203–210.

Simstich, J., et al. (2003), Paired delta O-18 signals of Neogloboquadrina pachyderma [s] and Turborotalita quinqueloba show thermal stratification structure in Nordic Seas, *Mar. Micropaleontol.*, *48*, 107–125, doi:10.1016/S0377-8398 (02)00165-2.

Spero, H. J., and D. W. Lea (1996), Experimental determination of stable isotope variability in Globigerina bulloides: Implications for paleoceanographic reconstructions, *Mar. Micropaleontol.*, *28*, 231–246, doi:10.1016/0377-8398(96)00003-5.

United Nations Educational, Scientific and Cultural Organization (1980), Background papers and supporting data on the International Equation of State of Seawater 1980, *UNESCO Tech. Pap. Mar. Sci.*, *38*, 192 pp., Paris.

Vaughan, D. G., and C. S. M. Doake (1996), Recent atmospheric warming and retreat of ice shelves on the Antarctic Peninsula, *Nature*, *379*, 328–331, doi:10.1038/379328a0.

Volkmann, R. (2000), Planktic foraminifers in the outer Laptev Sea and the Fram Strait–Modern distribution and ecology, *J. Foraminiferal Res.*, *30*, 157–176, doi:10.2113/0300157.

H. Elderfield, Department of Earth Sciences, Cambridge University, Downing Street, Cambridge CB2 3EQ, UK.

I. R. Hall, School of Earth and Ocean Sciences, Main Building, Park Place, Cardiff University, Cardiff CF10 3YE, UK.

V. L. Peck, British Antarctic Survey, High Cross, Madingley Road, Cambridge CB3 0ET, UK. (vlp@bas.ac.uk)

R. Zahn, Institució Catalana de Recerca i Estudis Avançats, Institut de Ciència i Tecnologia Ambientals, Departament de Geologia, Universitat Autònoma de Barcelona, E-08193 Bellaterra, Spain.